DEPENDENCE OF ELASTIC MODULUS ON MICROSTRUCTURE IN 2090-TYPE ALLOYS

M. O' Dowd, W. Ruch, E. Starke, Jr.

JOURNAL DE PHYSIQUE
Colloque C3, supplément au n°9, Tome 48, septembre 1987

DEPENDENCE OF ELASTIC MODULUS ON MICROSTRUCTURE IN 2090-TYPE ALLOYS

M.E. O'DOWD[1], W. RUCH, and E.A. STARKE, Jr.

Department of Materials Science, University of Virginia, Charlottesville, VA 22901, U.S.A.

ABSTRACT

The Young's modulus, shear modulus and Poisson's ratio were determined using an ultrasonic pulse echo technique. Three commercially fabricated aluminum-copper-lithium alloys and an aluminum-lithium binary alloy were examined. The elastic properties were measured as a function of aging time, aging temperature, amount of stretching and testing direction. An increase in Young's modulus due to delta prime and T1 precipitation has been measured and treated quantitatively including precipitation kinetics. A significant decrease of about 5% in the modulus of elasticity was found in the peak age condition. This decrease can be attributed to precipitation of the T2 phase. The shear modulus behaves similar to Young's modulus while the Poisson's ratio remains unchanged. There is no significant orientation dependence of the elastic properties on testing direction despite the fact that a typical rolling texture was present.

INTRODUCTION

It is well established that the addition of lithium decreases the density and increases the elastic modulus (1-4). This paper examines the important parameters which influence the elastic modulus in commercially important aluminum-lithium alloys. These parameters include solid solution concentrations, their volume fractions, and orientation effects. Industry can implement these results to produce aluminum-lithium alloys which possess an optimum elastic modulus.

EXPERIMENTAL PROCEDURE

The alloys studied in this investigation were donated by the Reynolds Metals Company, Richmond, Virginia. The material was received as hot cross-rolled plate with a thickness of 12 mm. The compositions of the alloys are given in Table I. Alloy 73 is similar in composition to ALCOA's 2090.

The alloys were solution heat treated at 550°C for 30 minutes in a salt bath and cold water quenched (CWQ). All the samples, alloys 73, 81, 82 and the binary alloy were aged at 190°C for times from 10 minutes up to 300 hours. They were all examined in the unstretched condition. Alloy 73 was also examined in a 6% stretched condition.

(1) Naval Air Development Center, Warminster, Pennsylvania, U.S.A.

Samples were machined for ultrasonic measurement from the center of the plate. The samples were rectangular, about 12 x 7 x 5 mm^3 in dimensions. Longitudinal and transverse wave velocities were measured with a 10 MHz ultrasonic pulse echo equipment.

The elastic modulus, shear modulus, and Poisson's ratio were calculated using the following equations (5):

$$R = (V_t/V_\ell)^2 \quad \text{eq. 1}$$

$$P = (2*R-1)/(2*R-2) \quad \text{eq. 2}$$

$$G = V_t^2*D \quad \text{eq. 3}$$

$$E = D*V_\ell^2*((1+P)*(1-2*P)/(1-P) \quad \text{eq. 4}$$

R - Ratio of velocities squared
P - Poisson's ratio
G - Shear Modulus (GPa)
E - Elastic Modulus (GPa)
D - Density (g/cc)
V_t - Transverse velocity (m/sec)
V_ℓ - Longitudinal velocity (m/sec)

The density of each sample was measured using Archimedes principle. The density did not change upon aging within 0.02%.

Texture analysis of the alloys was performed using a Siemens texture goniometer, set up for the Schulz reflection technique. Pole figures were obtained from each sample.

Transmission electron microscopy was performed using a Phillips 400 (120Kev) instrument. Small angle x-ray scattering (SAXS) was performed at the National Laboratory in Oak Ridge, Tennessee with $CuK\alpha$ radiation. A Huber Guinier Camera with a quartz monochromator using Cu $K\alpha_1$ radiation was used in connection with the direct comparison method to determine volume fractions of second phases.

RESULTS AND DISCUSSION

The microstructure of alloys 73, 81 and 82 display an elongated flat grain structure due to rolling. Typical dimensions are 220 x 100 x 30 μm^3. In addition there is a subgrain structure in the size range of 5 to 30 μm present. The binary alloy exhibited a fully recrystallized, equiaxed grain size ranging from 340 to 360 μm.

Figure 1 displays the results of TEM and Guinier x-ray analysis with respect to second phase precipitation at 190°C as a function of aging time. In the solution heat treated condition the matrix, δ' and Al_3Zr dispersoids were evident in the ternary alloys. The latter change neither distribution nor volume fraction during aging.

After 10 minutes aging at 190°C there is evidence of the T1 phase in alloy 73, but not in alloys 81 or 82. This can be explained by the higher Cu content of 73 resulting in a stronger driving force for T1 precipitation. The T1 phase nucleates heterogeneously at grain and subgrain boundaries. The platelets, after 10 minutes aging at 190°C, are approximately 72 nm long and 8 nm wide.

After approximately 90 minutes aging time the T1 phase is apparent in all three alloys. After 8 hours aging at 190°C, there is present in all three alloys some T2 phase which nucleates preferentially along the grain boundaries.

The volume fraction of δ' as a function of aging time was examined for alloy 81.

Table II shows that the direct comparison method yielded more consistent results than the TEM method. In the former method the integrated intensity ratio of the (200) and (100) diffraction line was measured from a Guinier camera exposure compared to the calculated value and solved for the volume fraction. At short aging times the superlattice line was too weak to be measured quantitatively and therefore a SAXS Kratky plot was used.

Figure 2 shows the δ' volume fraction in alloy 81 as a function of aging time. The SAXS data points (asterisks) have been calibrated with the direct comparison results (circles) at 40 min. aging time.

It is evident from Guinier camera and TEM results that the delta prime volume fraction remains essentially constant at longer aging times. SAXS data in Figure 2 shows an increase in volume fraction of second phases beyond 100 min., caused by T1 and T2 precipitation. The interpretation of the SAXS data in a more quantitative way is restricted due to the complicated shape and structure of T1 and T2. All ternary alloys exhibit the same (110)[$1\bar{1}2$] type texture (Figure 3). The maximum times random number of the (200) pole was 11, 7 and 10 for alloys 73, 81 and 82, respectively.

Figure 4 shows the Young's Modulus of the binary alloy as a function of aging time at 190°C. It exhibits an increase in the elastic modulus up to approximately 80 minutes aging time. The maximum modulus is approximately 80 GPa. 1 GPa is the largest overall change in modulus measured for the binary alloy where δ' and solid solution are the only phases present.

The elastic modulus versus aging time at 190°C for the ternary alloys in the unstretched condition, longitudinal direction is given in Figure 5. They reach a maximum elastic modulus at approximately 10 hours aging at 190°C. The maximum modulus of alloy 73 is 82 GPa. Alloys 81 and 82 reach a maximum modulus of approximately 80 GPa.

The shear modulus exhibits the same trends as the Young's modulus (see Figure 6). The values ranged from 29 to 31 GPa. The Poisson's ratio measurements did not exhibit any significant variation as a function of aging time. The values ranged between 0.30 and 0.33.

The variation in the elastic modulus exhibited by these alloys can be explained by changes in the microstructure. During aging, the grain size, grain orientation (texture) and density remain unchanged. Therefore, the precipitation of second phases is responsible for the changes in elastic behavior.

The change in modulus of 1 GPa exhibited by the binary alloy is due to the increasing volume fraction of delta prime. Beyond 100 minutes aging the volume fraction of delta prime remains constant. Coarsening of the delta prime has no measurable effect on the Young's modulus. This has also been reported by Broussaud and Thomas (6).

A volume fraction of 12.6% delta prime was determined using the Guinier camera on a sample which had been aged 200 hours. This corresponds well with a value of 11.5% calculated using the lever rule with the miscibility gap data reported by Cocco et al. (7).

Using a linear rule of mixtures the modulus of the delta prime can be calculated using the following equation:

$$E = f_{\delta'} E_{\delta'} + (1 - f_{\delta'})(E_{Al} + X C_{SS}^{Li}) \quad \text{. . . . . eq. 5.}$$

E - measured modulus
$f_{\delta'}$ - δ' volume fraction
$E_{\delta'}$ - modulus of delta prime
E_{Al} - modulus of aluminum
X - constant which depicts the dependence of the modulus of the matrix phase on the amount of lithium in solid solution.

C_{SS}^{Li} - Lithium concentration in solid solution (6.25 at% at metastable equilibrium)

E_{Al} and X have been determined by a linear regression of data reported by Muller et al. (8). They are 70.8 and 1.235, respectively. The modulus of delta prime calculated using the above equation with E = 80.7 GPa is 97 GPa. This value is reasonably close to 106 and 96 GPa reported elsewhere (6,8,9).

Equation 5 was also used to predict the change in modulus as a function of delta prime volume fraction. The lithium concentration in the solid solution (C_{SS}) can be related to the delta prime volume fraction according to the following equation:

$$C_{SS}^{Li} = (Y^{Li} - C_{SS}^{Li} f_{\delta'})/(1 - f_{\delta'}) \quad \ldots\ldots\ldots \text{ eq. 6}$$

Y^{Li} - total atomic fraction of lithium in the alloy

$C_{\delta'}^{Li}$ = 0.225 according to Cocco et al. (7).

Up to approximately 90 minutes aging, the unstretched ternary alloys can be treated as two phase materials comprised of the solid solution and delta prime phases. The aging kinetics of delta prime can be described using an equation from Turnbull (10):

$$f_{\delta'} = f_{\infty}(1 - (1 + B\ (t + t_o))^{-1/3} \quad \ldots\ldots\ldots \text{ eq. 7}$$

f_{∞} - equilibrium volume fraction
$f_{\delta'}$ - volume fraction of δ' at time, t
t_o - constant
B - constant.

This equation describes well the measured change in volume fraction of delta prime up to about 100 minutes aging time. The parameters used were f = 0.2, t_0 = 2.7705 min. and B = 0.3196 min^{-1}.

Using equations 5, 6, and 7 the change in modulus for alloy 81 aged up to where T1 begins to precipitate was calculated (see Figure 7). One can see that δ' precipitation has only a weak effect on the Young's modulus.

The increase in E beyond 90 minutes is caused by T1 precipitation. A T1 volume fraction of .7% was determined after 4 hours aging using the direct comparison method. Assuming a linear rule of mixtures the modulus of T1 can be calculated using the following equation:

$$E_{T1} = (E_{measured} - (f_{\delta'} E_{\delta'} + f_{SS} E_{SS}))/f_{T1} \quad \ldots \text{ eq. 8.}$$

Using constants from equation 5 for the modulus of the solid solution (E_{SS}) the T1 modulus calculates to about 350 GPa. This value is over two times higher than a rough approximation of the lower bound performed earlier (14).

The drop in E occurs at approximately 8 to 10 hours aging time with the precipitation of the icosahedral T2 phase. The data suggests that T2 has an extremely low intrinsic modulus because its volume fraction appears to be small. From Figure 2 follows that the volume fraction of delta prime at the longer aging times remains constant. This indicates that the T2 phase may grow somewhat at the expense of the T1 phase but not at the expense of delta prime. It may also take lithium out of solid solution, thus decreasing the modulus of the matrix phase even further.

The type of precipitates are the same in all three ternary alloys. However, the kinetics of precipitation are different. The

earlier onset of T1 precipitation in the high copper alloy, 73, shows up as an earlier increase in modulus and a larger difference between starting and peak modulus condition. The latter may be explained by a higher T1 volume fraction.

The modulus of alloy 73, stretched 6%, is 2 GPa lower than the unstretched material (Figure 8). This is due to the increased amount of dislocations in the stretched material which can result in anelastic strain effects thereby reducing the measured modulus. There is a more homogeneous precipitation of the T1 phase within the matrix at dislocation jogs (11). The increase in modulus in the stretched material occurs at a shorter age time due to the increase in the kinetics of precipitation.

Although we did not experimentally observe an influence of testing direction on the modulus, we calculated moduli for various testing directions from elastic constant data published by Muller et al. (8).

Linear regression analysis was performed to determine the elastic constants of our alloys. Using these elastic constant values the moduli are calculated and listed according to (12) in Table III, along with pure aluminum from reference (13).

The highest modulus, as expected, is in the [111] direction. The maximum theoretical difference in moduli due to testing direction (E_{max}) is only about half in aluminum-lithium alloys compared to pure aluminum. From a theoretical point of view the Al-Li solid solution alloys can be expected to be even more elastically isotropic than pure aluminum. Figure 9 shows that even during aging there is no directionality of the Young's modulus observable within experimental error despite the fact that a well pronounced rolling texture is present.

CONCLUSIONS

1. The Young's modulus increases only slightly due to the precipitation of delta prime (about 0.1 GPa/vol%).

2. The T1 phase contributes positively to the elastic modulus. Its intrinsic modulus is estimated to be approximately 350 GPa.

3. A maximum increase in E with aging time of approximately 5% can be attributed to the precipitation of T1, and to a lesser extent of δ', for the alloys examined.

4. There is a significant drop in the modulus at the peak aged condition (5%). It is associated with the precipitation of the T2 phase.

5. Al-Cu-Li alloys which have been stretched 6% will show a smaller, but faster increase in modulus upon aging. Earlier occurrence of the T1 phase and enhanced precipitation kinetics are responsible for this phenomenon.

6. There is no orientation dependence of the elastic modulus observed in these alloys.

ACKNOWLEDGEMENT

The authors would like to acknowledge the sponsorship of the Office of Naval Research, Grant #N00014-85-K0526, with Dr. Bruce MacDonald, program manager.

REFERENCES

1. E.A. Starke, Jr., T.H. Sanders, Jr., and I. Palmer, "New Approaches to Alloy Development in the Al-Li System," Journal of Metals 33 (1981) p. 24.

2. G.G. Wald, NASA Contractor Report 16576, Lockheed - California Company, Burbank, CA (May 1981).

3. W. Koster and W. Rauscher, Z. Metallkde 39 (1948) p. 111.

4. K.K. Sankaran and N.J. Grant: Aluminum-Lithium Alloys, eds. T.H. Sanders, Jr., and E.A. Starke, Jr., TMS-AIME, Warrendale, PA (1981) p. 205.

5. J. Krautkramer and H. Krautkramer, Ultrasonic Testing of Materials, 2nd ed., Springer-Verlag, New York (1977).

6. F. Broussaud and M. Thomas, "Influence of Delta Prime Phase Coalescence on Young's Modulus in an Al-2.5 wt% Li Alloy," Aluminum-Lithium Alloys III, eds. C. Baker, P.J. Gregson, S.J. Harris and C.J. Peel, Institute of Metals, London, UK (1986) p. 442.

7. G. Cocco, G. Fagherazzi and L. Schiffini, "Determination of the Delta Prime Coherent Miscibility Gap in the Al-Li System by Small-Angle X-ray Scattering," J. Appl. Cryst. 10 (1977) pp. 325-327.

8. W. Muller, E. Bubeck and V. Gerold, "Elastic Constants of Al-Li Solid Solutions and Precipitates," Aluminum-Lithium Alloys III, Institute of Metals, London, UK (1986), p. 435.

9. B. Noble, S.J. Harris, and K. Dinsdale, "The Elastic Modulus of Aluminum-Lithium Alloys," Journal of Materials Science 17 (1982) p. 461-468.

10. D. Turnbull, Solid State Physics 3 (1956) p. 226.

11. William A. Cassada, III, Ph.D. Thesis, University of Virginia, May 1987.

12. E. Kroner, Statistical Continuum Mechanics, Springer Berlin (1971).

13. C. Kittel, Introduction to Solid State Physics, 4th Edition, John Wiley and Sons, Inc., New York, NY (1971) p. 149.

14. E. Agyekum, W. Ruch, E.A. Starke, Jr., S.C. Jha and T.H. Sanders, "The Effect of Precipitate Type on the Elastic Properties of Al-Li-Cu and Al-Li-Cu-Mg Alloys", Aluminum-Lithium Alloys III, Institute of Metals, London, UK (1986) p. 448.

TABLE I. ALLOY COMPOSITIONS

ALLOY	wt% / at%	Al	Cu	Li	Zr	Cu/Li ratio
73	wt%	94.79	2.24	2.31	0.16	0.97
	at%	90.55	0.90	8.51	0.04	0.11
81	wt%	96.32	1.07	2.47	0.14	0.43
	at%	90.51	0.43	9.02	0.04	0.05
82	wt%	96.64	1.06	2.17	0.13	0.49
	at%	91.54	0.43	7.99	0.04	0.05
Binary	wt%	97.85		2.00		
	at%	92.60		7.36		

TABLE II. VOLUME FRACTION OF DELTA PRIME

Alloy	Age time at 190 C	TEM Method	Direct Comparison Method
		(vol%)	
81	4 hrs		11.2
81	8 hrs	7.0	
81	8 hrs	11.0	14.0
81	8 hrs	6.5	14.0
81	20 hrs		13.8
81	20 hrs		13.9
81	100 hrs		13.9

TABLE III. THEORETICAL MODULI FOR SOLID SOLUTIONS

Alloy	Crystallographic direction <hkl>				
	<111>	<110>	<100>	<112>	E_{max}(%)
82	83.60	81.38	75.38	81.38	11%
Al	75.30	71.73	62.81	71.73	20%

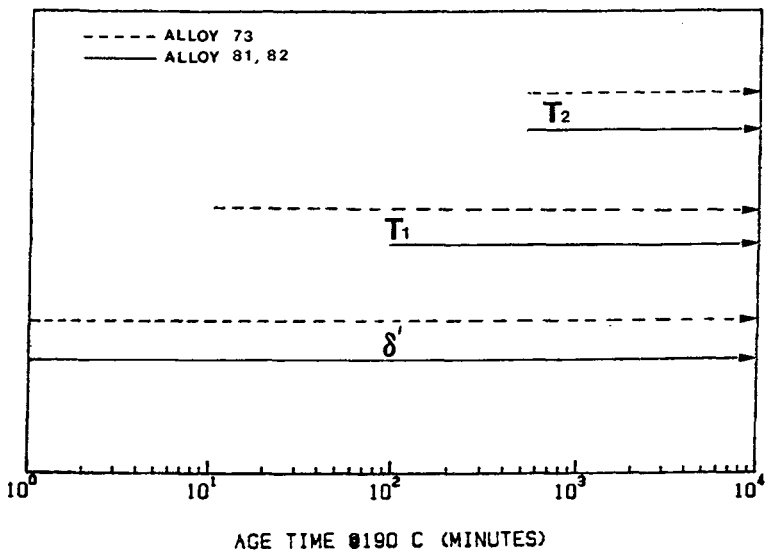

Figure 1. Profile of the occurrence of the delta prime, T1 and T2 phases in alloys 73, 81, and 82.

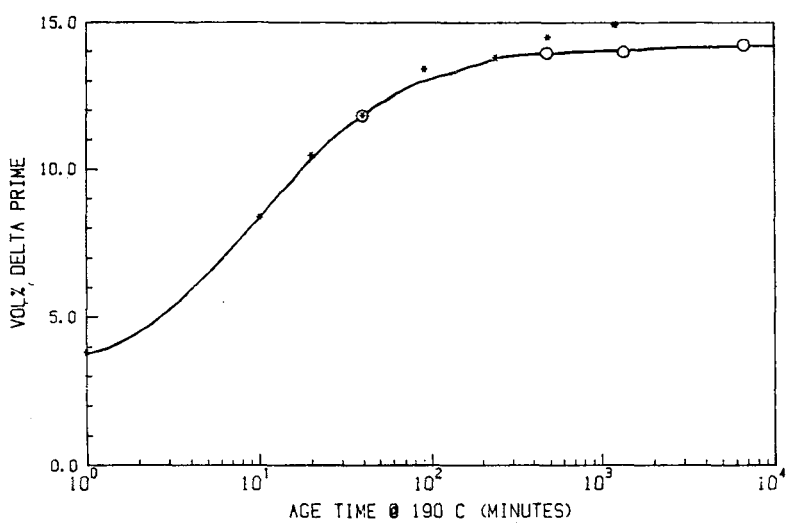

Figure 2. The volume fraction of delta prime in alloy 81 after aging at 190 C. (o) Guinier camera data; (*) SAXS data normalized.

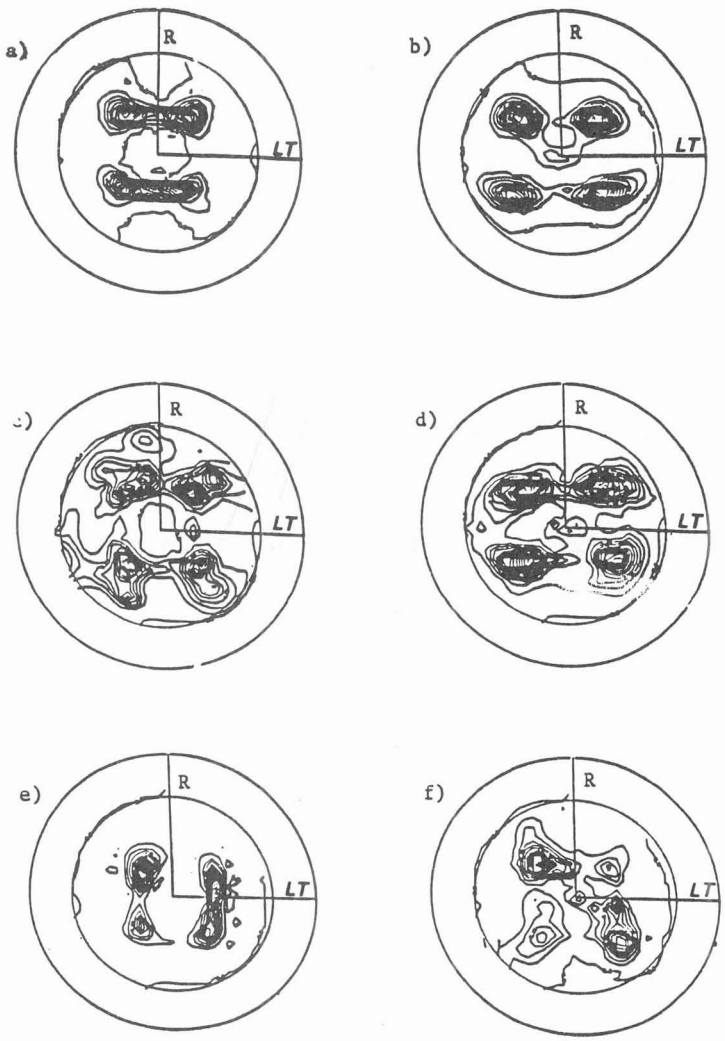

Figure 3. Pole figures a) Alloy 73 (111), b) Alloy 73 (200), c) Alloy 81 (111), d) Alloy 81 (200), e) Alloy 82 (111), and f) Alloy 82 (200).

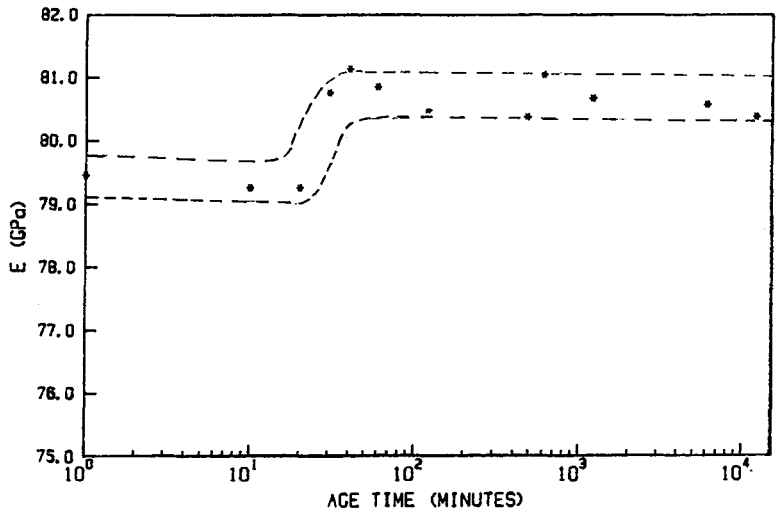

Figure 4. Elastic modulus versus aging time at 190°C of the binary alloy.

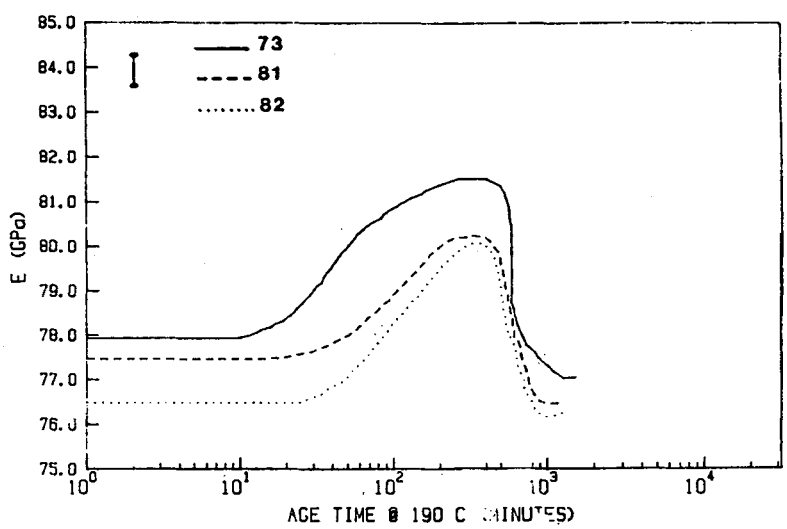

Figure 5. Young's modulus versus aging time at 190°C for alloys 73, 81 and 82 in the longitudinal testing direction.

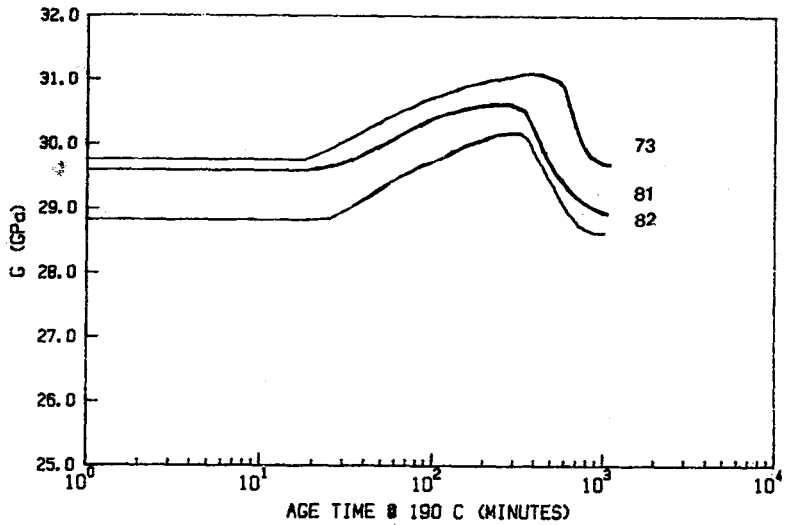

Figure 6. Shear modulus vs. aging time at 190°C for alloys 73, 81 and 82.

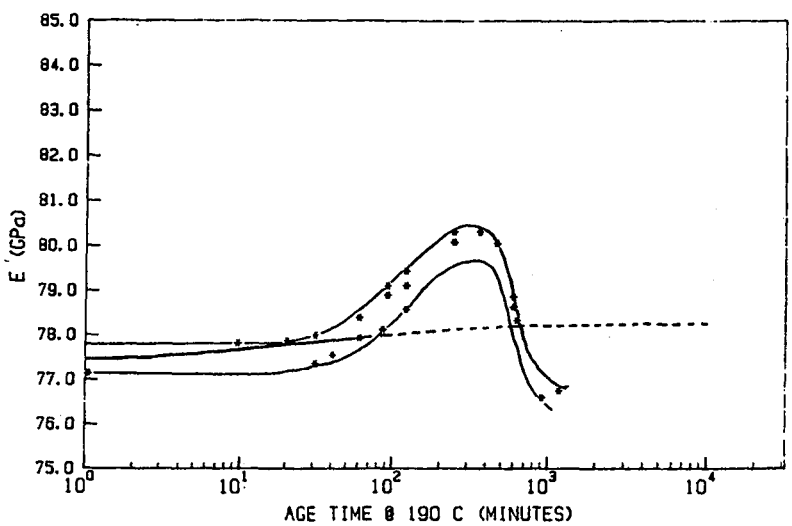

Figure 7. Elastic modulus versus aging time for alloy 81. Experimental data is compared with a theoretical prediction.

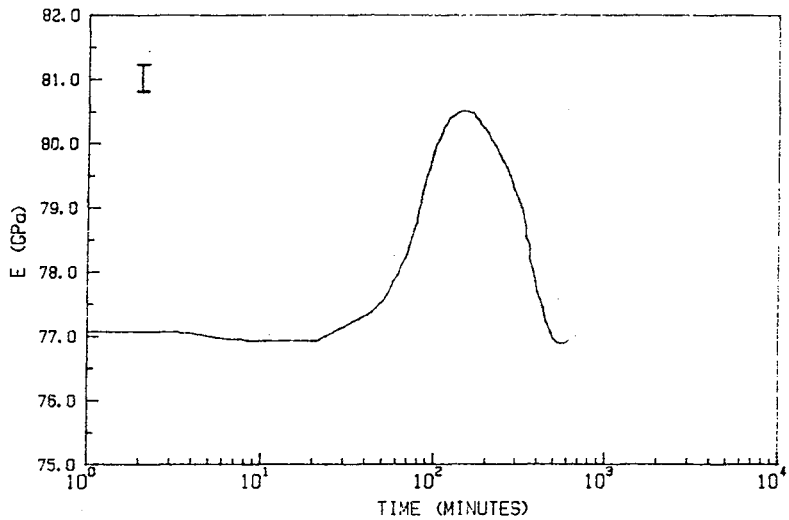

Figure 8. Young's modulus versus aging time at 190°C of alloy 73 stretched 6%.

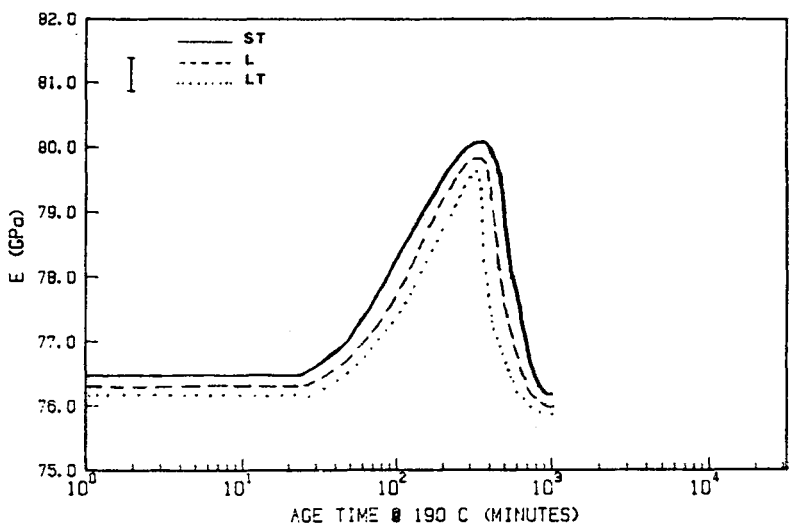

Figure 9. Young's modulus versus aging time at 190°C for the short transverse, long transverse and longitudinal directions of alloy 82.